Anal. Bioanal. Electrochem., Vol. 10, No. 3, 2018, 349-361

Analytical & Bioanalytical Electrochemistry

Full Paper

Effect of Sintering Temperature on the Pitting Corrosion of Ball Milled Duplex Stainless Steel by using Linear Sweep Voltammetry

Shashanka Rajendrachari*

Department of Chemistry, School of Engineering, Presidency University, Bengaluru-560064, India

*Corresponding Author, Tel.: +91 9449533539
E-Mail: shashankaic@gmail.com

Received: 17 September 2017 / Received in revised form: 16 February 2018 / Accepted: 14 March 2018 / Published online: 31 March 2018

Abstract- The nanostructured duplex stainless steel powders were prepared by specially designed dual drive planetary mill and their microstructural studies were carried out by using scanning electron microscope (SEM) and X-ray diffraction (XRD). The fabricated duplex stainless steels were consolidated by pressureless sintering method at 1100, 1200 and 1300 ˚C respectively at a load of 700MPa. Density, microhardness, microstructure and pitting corrosion of all the sintered duplex stainless steel samples were studied. The corrosion studies were carried out at 0.5, 1 and 2 M concentration of NaCl solution at different quiet time of 2, 6 and 10 seconds by linear sweep voltammetry (LSV) method. Duplex stainless steel samples sintered at 1300 ˚C shows better pitting corrosion resistance than the stainless steel samples consolidated at 1100 and 1200 ˚C. This is due to the improved densification with increase in sintering temperature. The microstructure of corroded duplex stainless steel samples were studied by using field emission scanning electron microscope (FESEM) and optical microscope.

Keywords- Stainless steel, Corrosion, Linear sweep voltammetry, Pitting potential, Planetary milling

1. INTRODUCTION

Duplex stainless steel is very important and popular stainless steels among all the other stainless steels due to their excellent corrosion resistant property, good high-temperature resistance, low thermal expansion, high tensile and creep strength [1]. Therefore it finds

applications as corrosion resistant super heaters, re-heaters, heat exchangers, bridges, desalination plants and high temperature boilers to improve their performances [2,3]. Author had reported the fabrication of nanostructured duplex stainless steel by high energy planetary ball mill in their previous publications [4,5]. Generally, duplex stainless steel possess good oxidation property, hence these can be used in fabricating high temperature components [6,7]. Duplex stainless steels prepared by powder metallurgy routes have lower oxidation properties at high temperature than the fully dense stainless steels fabricated by other methods [8]. Therefore, the porosity of these types of steels not only affect the surface area, density, hardness but also affect the quality of the protective oxide film formed on the surface of stainless steels [9]. Increase in the porosity results in the formation of poor quality protective film composed of iron and chromium oxide [10]. Many researchers had reported that, these types of stainless steels possess poor corrosion resistant properties than wrought steels due to high surface area [11-14]. To solve these problems many researchers all over the world trying to fabricate nanostructured duplex stainless steel by mechanical alloying. Because nanostructured materials impart improved typical properties [15,16]. The nanostructured duplex stainless steels not only show improved corrosion resistance but also exhibits improved densification and hardness. The improved corrosion resistance properties is due to the higher level diffusion of Cr and this in turn forms a dense protective layer on the surface of duplex stainless steel. In the present paper, we studied the corrosion resistance properties and microstructure of ball milled duplex stainless steel powders consolidated by pressureless sintering at different sintering temperatures.

Gupta et al. reported the preparation of mixture of nano and microcrystalline Fe-20Cr alloy powders by high energy ball milling followed by consolidation and studied their corrosion properties in acidic/acidic chloride solutions. They reported that the nano-crystalline alloy exhibits better corrosion resistant properties than microcrystalline alloys due to the greater Cr content in the passive film of nano-crystalline alloys [17].

Shankar et al. studied the pitting corrosion resistance of oxide dispersed stainless steel by cyclic polarization using 3.56 wt. % NaCl solution. They reported that, stainless steels sintered at 1250 °C exhibits better pitting corrosion resistant properties than the stainless steels sintered at 1400 °C [18]. J. Ahmed et al. fabricated Fe-18Cr-2Si alloy by mechanical alloying and consolidated the powders at different sintering temperatures (900, 1000 and 1100 ˚C). They successfully studied the effect of sintering temperature on the corrosion resistance properties of the stainless steel by using linear polarization resistance (LPR), potentiodynamic polarization (PDP) and electrochemical impedance spectroscopy (EIS) techniques. They reported that, the increased sintering temperature increases the corrosion resistance properties of stainless steel [8]. All the above techniques requires maximum time (around 1 h) to study the corrosion resistant properties, whereas, linear sweep voltammetry requires few seconds to determine the pitting corrosion of stainless steels. Usually most of

the corrosion studies were carried out by electrochemical methods such as impedance spectroscopy [19], polarographic methods [20], cyclic voltammetry [21] etc. As per author's knowledge no literature is available so far on the corrosion study of duplex stainless steel samples by linear sweep voltammetry (LSV) method. LSV is an important electrochemical technique involves solid electrode, fast scan and fixed potential. The slope of the ramp has units of volts per unit time and is generally called as scan rate of the experiment [22]. The results obtained by LSV method in the present study are comparable with the results obtained by impedance, polarographic methods [19,20]. The great advantage of using LSV is time required in determining the pitting potential of stainless steel is of the order of few seconds only and there is no need to keep stainless steel samples in NaCl or other electrolytes for many months to investigate the corrosion properties.

2. EXPERIMENTAL

2.1. Fabrication of nano structured duplex stainless steel by high energy ball mill

Nano-structured duplex stainless steel powders of composition Fe–18Cr–13Ni (wt. %) were prepared by dual-drive planetary mill (DDPM) under toluene atmosphere for 10 h. The entire milling experiments were carried out in DDPM consists of 1kg chrome steel balls with 8mm diameter and a steel jar of 1000 ml volume. The detailed mill fabrication and preparation of nano-structured duplex stainless steel powders were reported by authors in their previous publications [5,23]. The prepared stainless steel powders were characterized by X-ray diffraction (XRD) in a Philips PANalytical diffractometer using filtered Cu Kα-radiation (λ=0.1542 nm). The morphology of the stainless steel powders were studied by using scanning electron microscope (SEM).

2.2. Consolidation of nano-structured stainless steel powder by pressureless sintering

Ball milled duplex stainless steel powders were consolidated by pressureless sintering using hydraulic pressing machine at a load of 700 MPa using polyvinyl alcohol as binder. Generally, ball milled stainless steel samples have a wide range of crystallite sizes from micron- to nanolevel and hence it is difficult to compact powder samples without binder. The compacted pellets were sintered at 1100, 1200 and 1300 °C in argon atmosphere with holding time of 1 h each and samples were furnace cooled. The sintered pellets were polished carefully and their density and hardness were measured by Archimedes [24] and Vickers microhardness [25] methods respectively. Vickers microhardness studies were carried out using LECO-LM248AT fitted with a Vickers pyramidal diamond indenter. The hardness measurements were carried out at three different loads 10, 25 and 50 gf to study the effect of load on hardness with a dwell time of 10 seconds for all the trials and samples. The 5 trials of indentation of each sample were made with different loads and the average values of the diagonal lengths of indentation marks were measured.

2.3. Corrosion study by linear sweep voltammetry (LSV) method

The corrosion studies were carried out in a sophisticated three electrode electrochemical cell using electrochemical work station CHI-660 c model by LSV method. Potential scans were collected in a freely aerated NaCl solution of concentration 0.5, 1 and 2 M respectively at room temperature. All the consolidated stainless steel samples were polished to 4/0 grade finish and cleaned with distilled water before the experiment in each case. In the present paper we reported the effect of electrolyte concentration and the effect of sintering temperature on the pitting corrosion of duplex stainless steel. All the experiments were carried out in an electrochemical cell containing Ag/AgCl saturated KCl as reference electrode, stainless steel samples as working electrode (10 mm diameter) and platinum counter electrode. The microstructure of consolidated stainless steel samples were investigated by Carl Zeiss optical microscope and phase fractions of corroded duplex stainless steels were calculated by using Axio Vision Release 4.8.2 SP3 (08-2013) software.

3. RESULTS AND DISCUSSION

3.1. Characterization of nano-structured duplex stainless steel powders

3.1.1. Phase analysis by X-ray diffraction

X-ray diffraction spectra of nano-structured duplex stainless steel (Fe-18Cr-13Ni) powders milled for 0, 2, 5 and 10 h by DDPM are shown in fig. 1. Due to the frequent active collision of jar-powder-balls unceasingly inside the mill had made alloy powder with maximum internal strain, more defects and refined grain size [26,27].

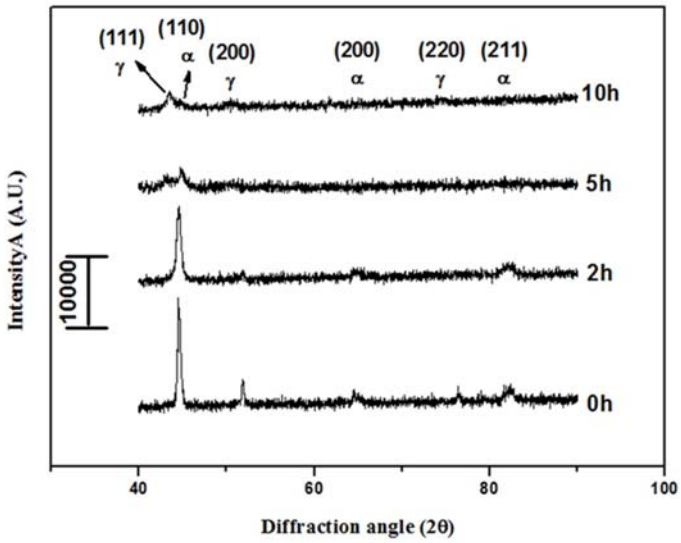

Fig. 1. XRD spectra of duplex stainless steel powder milled for 0, 2, 5 and 10 h respectively

At 0h, XRD peak is sharp and crystalline and gradually starts to broaden due to the refined crystallite size and increased lattice strain during milling. Nelson-Riley extrapolation method [5] was used to calculate lattice parameter value for 10 h milled duplex stainless steel and the value was found to be 3.51Å (matches with standard value 3.515 Å). Crystallite size and lattice strain of duplex stainless steel is calculated by Williamson-Hall method [5] and they are found to be 8 nm and 5.595×10^{-3} respectively. During milling, volume fractions of grain boundaries increases due to the phenomenon such as grain size reduction, structural defect and amorphization during milling. This results in the formation of shorter diffusion path, more defect storage sites and attains meta-stable non-equilibrium state [1,28]. From the graph it is clear that, duplex stainless steel at 10 h of milling shows more dominant austenite peaks than ferritic peaks, this confirms the phase transformation of α-Fe to γ-Fe.

3.1.2. Microstructure analysis by SEM

Fig. 2 represents the SEM micrographs of duplex stainless steel powders milled at different time intervals (0 to 10 h). It was found that, before milling the powder particles were large and irregular in shape; but as the milling proceeds, particles begin to agglomerate and become flat due to the ductile nature of Fe. Further increase in the milling time results in the welding of two or more flat lamellae together to form a single large lamella and ultimately the ductile powder particles get work hardened; Ni and Cr get entrapped into Fe lattice and powder particles begins to refine. This leads to the reduction in the particle size again and further refinement in the size of the particles becomes difficult beyond 10 h of milling.

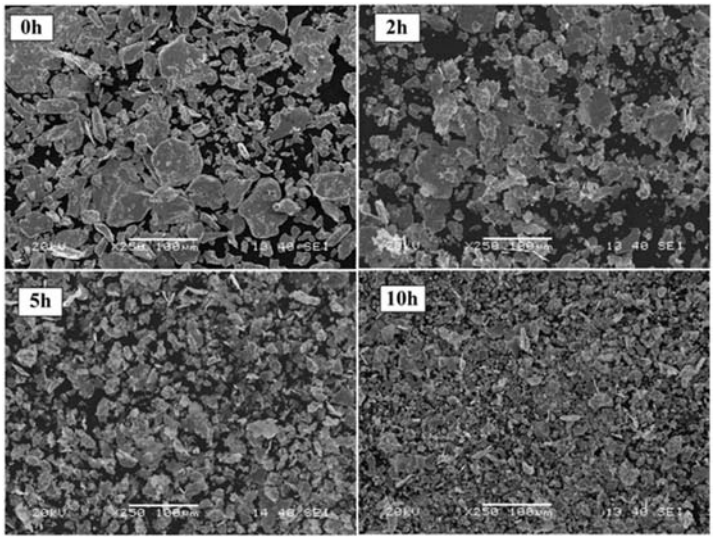

Fig. 2. SEM micrographs of duplex stainless steel powders milled at different time intervals (0 to 10 h)

It has been found that 10 h of milling leads to the formation of fine and spherical shaped stainless steel powder particles with uniform distribution of Ni and Cr in the solid solution of Fe. From the micrographs it was found that particle size of 10 h milled duplex stainless steel powder is around 5–10 μm.

3.2. Characterization of consolidated duplex stainless steel

3.2.1 X-ray diffraction study of stainless steel samples

Fig. 3 (a) shows X-ray diffraction patterns of duplex stainless steel samples consolidated at 1100, 1200 and 1300 ˚C respectively. XRD spectra of milled duplex stainless steel powder (fig. 1) shows broadened diffraction peaks of austenite and ferrite as limited transformation from ferrite to austenite during milling.

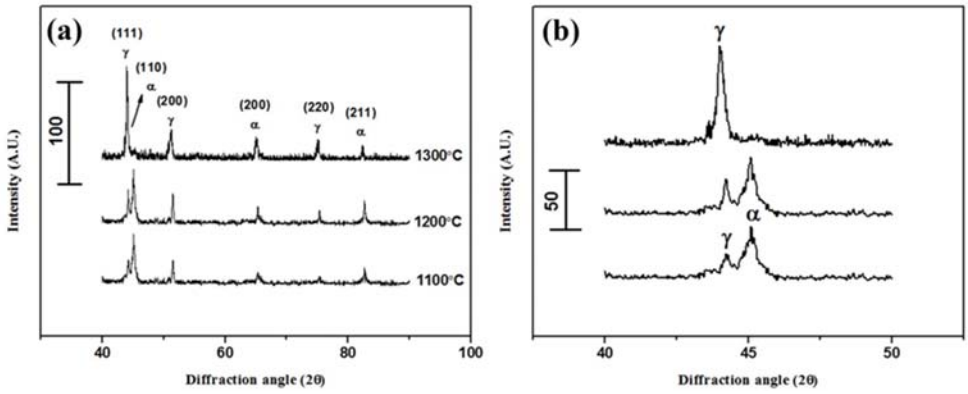

Fig. 3. (a) X-ray diffraction patterns of duplex stainless steel samples consolidated at 1100, 1200 and 1300 ˚C respectively; **(b)** The enlarge view (scan range 40–50°) of the first peak of duplex stainless steel

During milling, the stainless steel powder will undergo many transformations like structural defects; amorphization; reduction in crystallite size and increase in volume fraction of grain boundaries [1]. This increases the number of defect storage sites, shorter diffusion paths and attains non-equilibrium state as reported by Gojic et al. [29]. But after consolidation of duplex stainless steel, the XRD spectra shows sharp crystalline diffraction peaks of both austenite and ferrite. During consolidation, Cr and Ni move into the interstitial site of Fe lattice through diffusion process. Hence, strong peaks of ferrite and austenite are visible after consolidation. The sharpness and crystallinity of diffraction peaks increases with increase in sintering temperature from 1100 to 1300 °C as shown in the fig. 3 (a). This is due to the atomic diffusion through nicking and rearrangement of the particles in a regular manner and increases the crystallinity of stainless steel. The diffusion rate, grain growth and the atomic periodicity increases with increasing sintering temperature as shown in the figure.

Fig. 3 (b) shows the enlarge view (scan range 40–50°) of the first peak in inset. It shows the diffraction peaks of both austenite and ferrite; and the diffraction peak is shifting towards lower diffraction angle; this confirms the phase transformation of ferritic to austenitic stainless steel at higher sintering temperatures. There are no diffraction peaks of secondary phases like sigma phase; carbides or nitrides precipitations in both powders as well as consolidated duplex stainless steel samples.

3.2.2. Microstructure and phase analysis

Fig. 4 shows the optical micrographs of duplex stainless steel samples consolidated at 1100, 1200 and 1300 °C respectively.

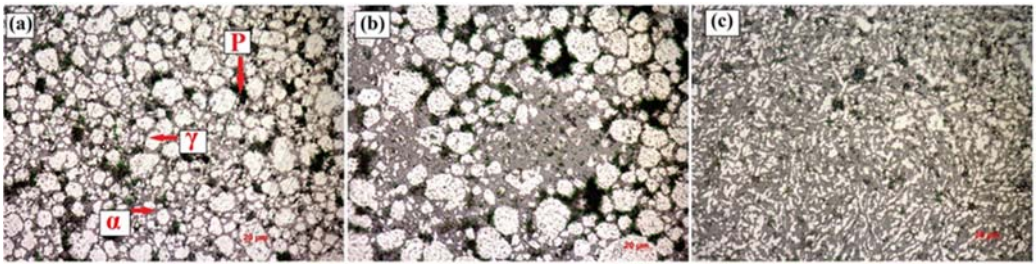

Fig. 4. Optical microstructure of duplex stainless steel samples sintered at 1100, 1200 and 1300 °C in argon atmosphere (P- Pores)

From the optical micrographs it is confirmed that, as the sintering temperature increases from 1100 to 1300 ˚C; density increases and number of pores decreases. This is due to the release of strain, decrease in defect storage sites, grain growth and increase in crystallinity due to the diffusion of atoms to form a regular cubic geometry. XRD spectra of Figure 3 (a) can also confirms the formation of more dominant austenite peaks at higher sintering temperatures. Therefore, we have carried out an investigation to study the extent of volume fraction of ferrite and austenite phase in duplex stainless steel at different sintering temperatures. The volume fractions of both ferrite and austenite phases were calculated by Axio Vision Release software. From these results we can concluded that, the amount of austenite phase increases with increase in sintering temperature from 1100 to 1300 °C due to the phase transformation of ferrite to austenite at higher temperatures. Amount of austenite phase has been increased from 52 to 68 volume fractions during sintering from 1100 to 1300 °C. In the micrographs, ferrite (α-Fe), austenite (γ-Fe) and pores (P) are shown.

3.2.3. Density and hardness study

Fig. 5 (a) depicts the effect of temperature on the densities of duplex stainless samples consolidated by pressure less sintering. The density of the stainless steel samples increases and porosity ratio decreases with an increase in sintering temperature from 1100 to 1300 ˚C as shown in the figure.

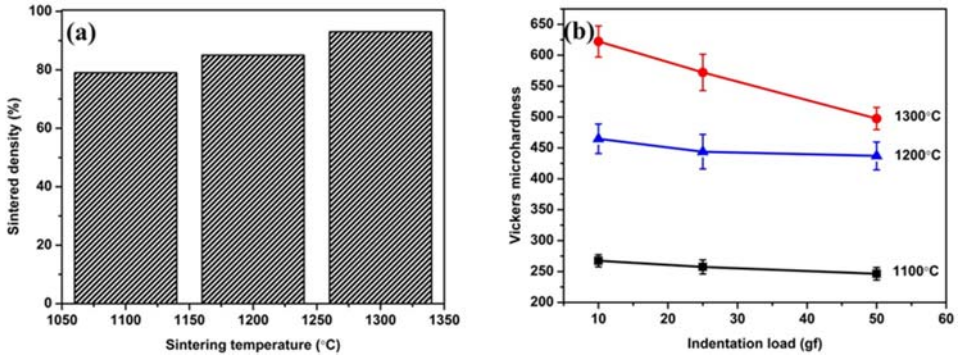

Fig. 5. Graph of **(a)** Sintered density **(b)** Vickers microhardness versus indentation load (10, 25 and 50 gf) of duplex stainless steel samples sintered at 1100, 1200 and 1300 °C in argon atmosphere

A maximum density of 90% was achieved for the stainless steel samples sintered at 1300 °C. Average hardness values of duplex stainless steels at 1100, 1200 and 1300 °C are shown in Fig. 5 (b) and the values obtained are high compared with previous literatures [4]. Density, hardness and volume fractions of austenite and ferrite phases in duplex stainless steel at different sintering temperatures are tabulated in Table 1.

Table 1. Volume fractions, density and hardness of austenite and ferrite phases of duplex stainless steel samples sintered in argon atmosphere at different sintering temperature

Sample	Sintering Temperature (°C)	Volume fraction (%)		Theoretical density (g/cc)	Sintered density (%)	Vickers microhardness (HV)
		Austenite phase	Ferrite Phase			
Duplex stainless steel	1100	55	45	7.84	79	254
	1200	61	39		85	443
	1300	67	33		93	570

It was observed that, microhardness values decreases with an increase in applied indentation load. This is due to the indentation size effect (ISE) [30] and this in turn directly

related to the intrinsic structural factors of the test materials such as indentation elastic recovery; work hardening during indentation; surface dislocation pining [31,32]; surface effect; strain gradient effect and non-dislocation mechanisms based on mass transport by point defects [33]. Microhardness values of duplex stainless steel consolidated at 1100, 1200 and 1300 °C were found to be 254, 443 and 570 HV respectively at 25 gf. Both microhardness and density of duplex stainless steel samples increases with an increase in sintering temperature from 1100 to 1300 °C. This is due to the low porosity ratio and maximum amount shrinkage at higher sintering temperature. The rate of mass transport increases with increase in sintering temperature and eventually results in the formation of neck and better bonding between powder particles [4,34,35].

3.3. Corrosion study by linear sweep voltammetry (LSV) method

We reported the effect of quiet time (reaction time), sintering temperature and the effect of different concentration of NaCl electrolyte on pitting corrosion of duplex stainless steel consolidated by pressure less sintering method. The NaCl electrolytes of concentrations 0.5, 1 and 2 M were prepared in double distilled water and used to study the pitting corrosion. The duplex stainless steel whose corrosion properties to be studied was made as working electrode and kept inside the electrochemical cell containing NaCl electrolyte, counter electrode and reference electrode. Pitting corrosion experiments were performed by using LSV at a sweeping potential from 0.9 to 0 V (adjusted according to the pitting potential) with different quiet time from 2, 6 and 10 seconds. A current-potential curve is obtained for each individual quiet time at constant concentration. Fig. 6 represents the linear sweep voltammetric curve of duplex stainless steel samples at 0.5 M NaCl electrolyte at different quiet time. As the potential sweeps from 0.9 to 0 V the sharp increase in current can be observed at a particular potential and that potential is called as pitting potential (E_P). The sharp increase in current is due to the availability of more electrons after depleting Cr_2O_3 passive layer and this result in pitting and it grows further if the metal is unprotected.

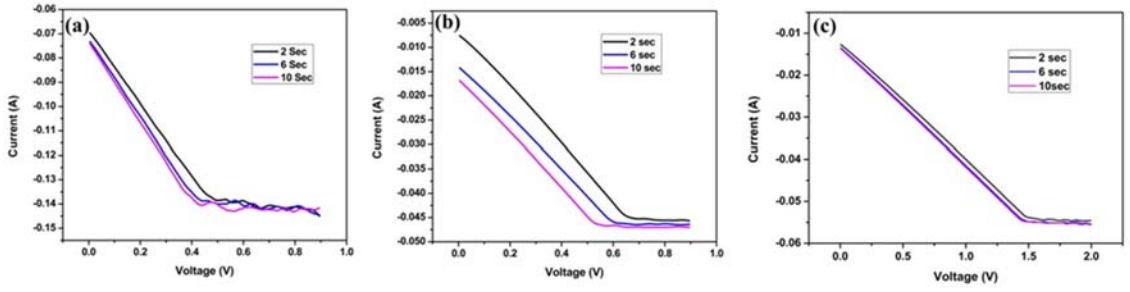

Fig. 6. Potentiometric curves duplex stainless steel consolidated at **(a)** 1100 °C **(b)** 1200 °C and **(c)** 1300 °C in 0.5 M NaCl solution at different quite time (2 to 10 seconds)

The following reactions are responsible for corrosion in duplex stainless steel at NaCl electrolyte,

Anodic reaction: $Fe \longrightarrow Fe^{2+} + 2e^{-}$ (Dissolution of Iron)

$Fe^{2+} + 2H_2O \longrightarrow FeOH^{+} + H_3O^{+}$

Formation of $FeOH^{+}$ is mainly responsible for the sudden increase in current due to the dissolution of Fe metal.

Cathodic reaction: $O_2 + 2H_2O + 4e^{-} \longrightarrow 4OH^{-}$

Main reaction: $Fe^{2+} + 2Cl^{-} \longrightarrow FeCl_2$

$FeCl_2 + 2H_2O \longrightarrow Fe(OH)_2 + 2HCl$

Formation of $Fe(OH)_2$ decreases the pH of the electrolyte inside a pit from 6 to 2, which induces further corrosion process [36].

The pitting corrosion process is evidenced by the LSV measurement method by sudden and drastic increase in pitting current (I_P). The pitting current value goes on decreasing with increase in sintering temperature from 1100 to 1300 ˚C as shown in the Fig. 7. This is due to the reduced porosity ratio at higher sintering temperature and the improvement in oxidation properties; diffusion of Cr and the ease of passive layer formation at higher sintering temperature. There is no formation of secondary phases like sigma phase; carbides or nitrides precipitations in consolidated duplex stainless steel samples as these phases have negative effect on pitting corrosion of stainless steel. Stainless steel sintered at high temperature possesses higher degree of Cr diffusivity and a very dense and strong Cr_2O_3 passive layer [8], hence more potential is required to break down the oxide layer. Higher the pitting potential more is the corrosion resistance [37].

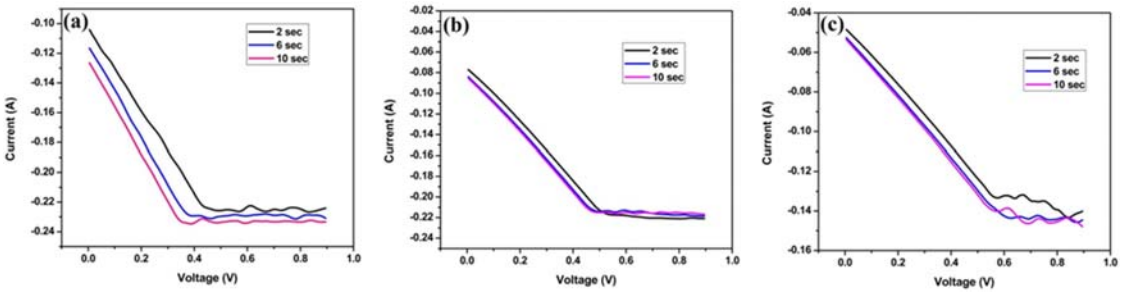

Fig. 7. Potentiometric curves duplex stainless steel consolidated at **(a)** 1100 °C **(b)** 1200 °C and **(c)** 1300 °C in 1 M NaCl solution at different quite time (2 to 10 seconds)

Fig. 7 and Fig. 8 represents the linear sweep voltammetric curves of duplex stainless steel samples at 1 M and 2 M NaCl concentrations respectively at different quiet time. The E_P value of duplex stainless steel samples sintered at 1100, 1200 and 1300 ˚C in 0.5 M NaCl concentration with 6 sec quite time was found to be 0.43 V, 0.6 V and 1.4 V respectively.

Similarly stainless steel samples sintered at 1100, 1200 and 1300 ˚C in 1 M and 2 M NaCl concentrations with 6 sec quite time were found to have E_P values of 0.38 V, 0.47 V, 0.62 V; and 0.20 V, 0.24 V, 0.47 V respectively. From the voltammograms it is clear that as the concentration of NaCl electrolyte increases from 0.5 to 2 M then pitting potential for duplex stainless steel samples decreases due to the accelerated rate of corrosion reactions at higher concentrations.

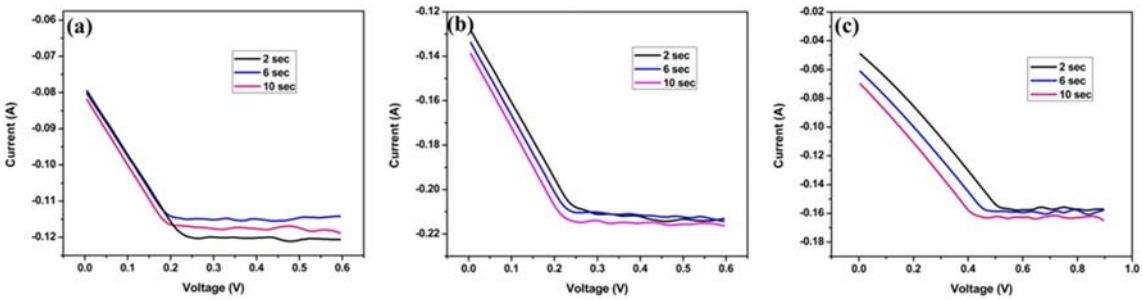

Fig. 8. Potentiometric curves duplex stainless steel consolidated at **(a)** 1100 °C **(b)** 1200 °C and **(c)** 1300 °C in 2 M NaCl solution at different quite time (2 to 10 seconds)

3.3.1. Microstructural analysis of stainless steel samples after corrosion study

Fig. 9 (a) depicts the FESEM image of duplex stainless steel samples (sintered at 1300 ˚C) corroded in 0.5 M NaCl solution.

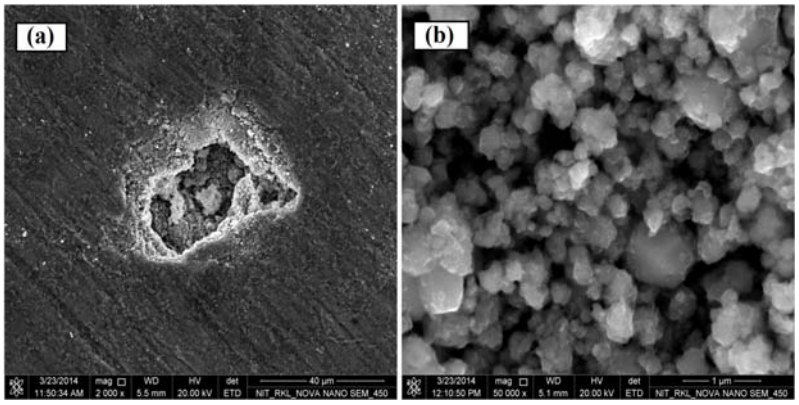

Fig. 9. (a) FESEM images of duplex (sintered at 1300 ˚C) corroded in 0.5 M NaCl concentration; **(b)** High resolution image of corroded region inside the pit

From FESEM images of duplex stainless steel one can observe white regions; these white regions confirm the oxidation reactions during electrochemical measurement. Fig. 9 (b) depicts the high resolution image of corroded region inside the pit; the spherical white granules are oxides of iron confirming the process of corrosion.

4. CONCLUSION

Nano-structured duplex stainless steel powders were prepared at different time intervals by using DDPM. Fabricated duplex stainless steel powders were consolidated by pressureless sintering in a tubular furnace at 1100, 1200 and 1300 °C at a load of 700 MPa under argon atmosphere for 1 h each. XRD and Microstructural analysis were performed for consolidated stainless steel samples before corrosion study. X-ray diffraction analysis confirms the phase transformation of ferritic to austenitic stainless steel at higher sintering temperatures. The density and microhardness of the duplex stainless steel samples increases with increase in sintering temperature from 1100 to 1300 ˚C. We successfully studied the pitting corrosion properties of consolidated stainless steel samples by LSV method at different concentration of NaCl solution. As the concentration of NaCl solution increases from 0.5 to 2 M then pitting potential decreases due to the accelerated rate of corrosion reactions at higher concentrations. Similarly, duplex stainless steel samples sintered at higher temperatures imparts maximum pitting corrosion resistance.

REFERENCES

[1] R. Shashanka, and D. Chaira, Powder Technol. 278 (2015) 35.
[2] S. Gupta, R. Shashanka, and D. Chaira, IOP Conference 75 (2015) 012033.
[3] S. Herenu, I. A. Armas, and A. F. Armas, Scripta Materialia 45 (2001) 739.
[4] R. Shashanka, and D. Chaira, Powder Technol. 259 (2014) 125.
[5] R. Shashanka, and D. Chaira, Mater. Charact. 99 (2015) 220.
[6] A. Bautista, A. G. Centeno, G. Blanco, and S. Guzman, Mater. Charact. 59 (2008) 32.
[7] P. Samal, and J. Terrell, Met. Powder Rep. 56 (2001) 28.
[8] J. Ahmed, I. H. Toor, and N. Al-Aqeeli, Materials and Corrosion. 68 (2017) 361.
[9] A. G. Centeno, F. Velasco, A. Bautista, and J. M. Torralba, Mater. Sci. Forum. 426–4 (2003) 4355.
[10] A. Bautista, C. Moral, F. Velasco, C. Simal, and S. Guzman, J. Mater. Process. Technol. 189 (2007) 344.
[11] E. Otero, A. Pardo, M. Utrilla, E. Saenz, and J. Alvarez, Corr. Sci. 40 (1998) 1421.
[12] E. Otero, A. Pardo, E. Saenz, M. V. Utrilla, and P. Hierro, Corr. Sci. 38 (1996) 1485.
[13] T. Raghu, S. N. Malhotra, and P. Ramakrishnan, Corrosion. 45 (1989) 698.
[14] L. Fedrizzi, J. Crousier, P. L. Bonora, and J. P. Crousier, Werkstoffe und Korrosion 42 (1991) 403.
[15] R. Shashanka, B. E. K. Swamy, S. Reddy, and D. Chaira, Anal. Bioanal. Electrochem. 5 (2013) 455.
[16] S. Reddy, B. E. K. Swamy, S. Aruna, M. Kumar, R. Shashanka, and H. Jayadevappa, Chemical Sensors. 2 (2012) 1.

[17] R. K. Gupta, R. K. S. Raman, C. C. Koch, and B. S. Murty, Int. J. Electrochem. Sci. 8 (2013) 6791.
[18] J. Shankar, A. Upadhyaya, and R. Balasubramaniam, Corros. Sci. 46 (2004) 487.
[19] J. Chen, R. M. Asmussen, D. Zagidulin, J. J. Noel, and D. W. Shoesmith, Corros. Sci. 66 (2013) 142.
[20] C. X. Li, and T. Bell, Corros. Sci. 48 (2006) 2036.
[21] M. M. Hukovic, R. Babic, Z. Grubac, Z. Petrovic, and N. Lajci, Corros. Sci. 53 (2011) 2176.
[22] Basics of Voltammetry and Polarography, Princeton Applied Research, Applied Instruments Group, Application Note p-2.
[23] A. K. Nayak, R. Shashanka, and D. Chaira, IOP Conference 115 (2016) 012008.
[24] R. Shashanka, and D. Chaira, Tribology Transaction 60 (2017) 324.
[25] R. Shashanka, and D. Chaira, Acta Metall. Sin. (Engl. Lett.). 29 (2016) 58.
[26] R. Shashanka, D. Chaira, and B. E. Kumara Swamy, Int. J. Scient. Eng. Res. 6 (2015) 1863.
[27] R. Shashanka, D. Chaira, and B. E. Kumara Swamy, Int. J. Scient. Eng. Res. 7 (2016) 1275.
[28] R. Shashanka, D. Chaira, and B. E. Kumara Swamy, Int. J. Electrochem. Sci. 10 (2015) 5586.
[29] M. Gojic, A. Nagode, B. Kosec, S. Kozuh, S. Savli, T. H. Grguric, and L. Kosec, Eng. Failure Anal. 18 (2011) 2330.
[30] R. Shashanka, D. Chaira, and D. Chakravarty, J. Mater. Sci. Eng. B 6 (2016) 111.
[31] J. Gong, Wu. Jianjun, and Z. Guan, J. Eur. Ceram. Soc. 9 (1999) 2625.
[32] I. H. Buckle, Use of the hardness test to determine other material properties, in: J.H. 24 Westbrook, H. Conrad (Eds.), The Science of Hardness Testing and Its Research 25 Application, American Society for Metals., Metal Park, Ohio, (1973) 453.
[33] I. Manika, and J. Maniks, Acta Mater. 54 (2006) 2049.
[34] R. Shashanka and D. Chaira, Ball Milled Nano-Structured Stainless Steel Powder: Synthesis and Characterization. Educreation Publishing, 2017. ISBN: 978-1-5457-0821-7.
[35] R. Shashanka, Int. J. Scient. Eng. Res. 8 (2017) 588.
[36] F. Y. Ma, Corrosive effects of Chlorides on Metals, Pitting Corrosion, Prof. Nasr Bensalah (Ed.), ISBN: 978-953-51-0275-5, InTech (2012).
[37] E. B. Tamarit, D. M. García-Garcia, and J. Garcia Anton, Corros. Sci. 53 (2011) 784.